Clinical Biomechanics 53 (2018) 117–123

Contents lists available at ScienceDirect

Clinical Biomechanics

journal homepage: www.elsevier.com/locate/clinbiomech

Shoulder mechanical demands of slow underwater exercises in the scapular plane

Jessy Lauer[a,b,*], João Paulo Vilas-Boas[b], Annie Hélène Rouard[a]

[a] *Inter-university Laboratory of Human Movement Science, University Savoie Mont Blanc, Le Bourget-du-Lac, France*
[b] *Center of Research, Education, Innovation and Intervention in Sport, Faculty of Sport and Porto Biomechanics Laboratory, University of Porto, Porto, Portugal*

A R T I C L E I N F O

Keywords:
Aquatic therapy
Load
Inverse dynamics
Joint kinetics

A B S T R A C T

Background: The mechanical demands of underwater shoulder exercises have only been assessed indirectly via electromyographical measurements. Yet, this is insufficient to understand all the clinical implications. The purpose of this study was to evaluate musculoskeletal system loading during slow (30°/s) scapular plane arm elevation and lowering performed in two media (air vs water) and body positions (sitting vs supine).
Methods: Eighteen participants' upper bodies were scanned and virtually animated within unsteady numerical fluid flow simulations to compute hydrodynamic forces. Together with weight, buoyancy and segment inertial parameters, these were fed into an inverse dynamics model to obtain net shoulder moments, power and work.
Findings: Positive mechanical work done at the shoulder was 32.4% (95% CI [29.2, 35.6]) and 25.0% [22.8, 27.2] that when performing the same movement on land, supine and sitting respectively. Arm elevation was ~2.5× less demanding sitting than supine (mean 0.012 (SD 0.018) vs mean 0.027 (SD 0.012) $J{\cdot}kg^{-1}$, $P = 0.034$). Instantaneous power was consistently positive when sitting albeit very low during elevation (0.003 $W{\cdot}kg^{-1}$) whereas, when supine, it was alternately negative for short period (~1.2 s) and positive (~4.8 s), peaking at levels 3× higher (0.01 $W{\cdot}kg^{-1}$).
Interpretation: Performing sitting elicited concentric muscle contractions at very low effort, which is advantageous during early rehabilitation to restore joint mobility. Exercising supine, by contrast, required rapid prestretch followed by concentric force production at an overall higher mechanical cost, and is therefore better suited to more advanced rehabilitation stages.

1. Introduction

Rotator cuff disorders, regarded as the principal cause of shoulder pain and upper extremity disability, rank among the most common musculoskeletal conditions. In France, about 128 surgical operations on average have been performed daily for the past 3 years (ATIH, 2017). Protecting the postoperative shoulder from excessive load is vital, particularly early in the rehabilitation process. In that context, aquatic therapy provides formidable potential benefits. Thanks to buoyancy, the upward thrust that counteracts the action of gravity, water offers near-weightlessness exercise conditions. This unique physical property significantly accelerates the restoration of shoulder flexion range of motion as early as three weeks post-surgery (Brady et al., 2008). Furthermore, water is very viscous and thus highly dampening. Resistance rapidly decays upon cessation of movement, which is thought to dramatically reduce the risk of reinjury (Prins and Cutner, 1999).

The latest American Society of Shoulder and Elbow Therapists' consensus promotes the use of slow (30°/s) aquatic scapular plane movements to initiate aquatic therapy (Thigpen et al., 2016). The guideline is based on the observation that, at that speed, the electromyographical (EMG) activity of the deltoid and rotator cuff muscles was on average ~2–5× lower in water than on land (Castillo-Lozano et al., 2014; Kelly et al., 2000). Assuming load was proportional to muscle activity, the authors concluded that slow underwater shoulder exercises were likely safe enough for early active mobilization. However, EMG recordings only offer insight into individual muscle activation level and are poor indicators of the mechanical load on the musculoskeletal system (Winby et al., 2013; Zajac et al., 2002).

Internal load is best estimated noninvasively from inverse dynamics (van den Bogert, 1994). On land, the procedure requires the knowledge of segment inertial properties, linear and angular accelerations, as well as the ground reaction force. Eventually, it yields mechanical quantities that are superior to EMG in their capacity to analyze how muscle groups meet task mechanical requirements. Joint moments, for example, identify the dominant musculature during the observed motion (Desroches et al., 2010), and can, under different conditions, be

* Corresponding author at: LABIOMEP, Rua Dr. Plácido Costa 91, 4200–450 Porto, Portugal.
E-mail address: jessy.lauer@gmail.com (J. Lauer).

https://doi.org/10.1016/j.clinbiomech.2018.02.014
Received 25 June 2017; Accepted 22 February 2018

representative of muscle force production and ligament loading (Kristianslund et al., 2014). The calculation of joint work, on the other hand, provides a reasonable evaluation of the actual work produced by muscles during slow movement (Sasaki et al., 2009). As such, it is a more objective and meaningful criterion of internal loading than EMG. Remarkably, inverse dynamics also has the potential to unveil the type of dynamic muscle action through the computation of joint power (Robertson and Winter, 1980). Nonetheless, a thorough inverse dynamics analysis of shoulder loading in water has never been reported. Unlike on land, accurate measurements of the hydrodynamic forces acting upon the entire upper limb surface and their respective points of force application are needed—this makes the process very complex and one of the major challenge of aquatic therapy (Biscarini and Cerulli, 2007).

A new methodology coupling inverse dynamics with numerical fluid flow simulations has been recently proposed to calculate instantaneous internal loading (Lauer et al., 2016). Armed with these new tools, it is also now possible, in addition to the quantities described above, to dissect the mechanical effects of buoyancy, weight, and water resistance. It is believed that modulating the action of buoyancy on the upper limb possibly influences the work done at the shoulder (Thein and Brody, 2000). This hypothesis is best viewed from a simple mechanical analysis of identical movements performed in two different positions. When sitting, buoyancy assists scapular plane arm elevation and resists arm lowering. On the other hand, buoyancy alternates between both roles when supine, temporarily assisting then resisting motion. However, the extent to which changes in body position alter shoulder load, and whether this may compromise therapy success, must be clarified.

We therefore sought to evaluate the shoulder mechanical demands of scapular plane movements performed at 30°/s in water and on land, while supine and sitting. Based on past EMG findings, we expected load in water to be roughly within 20–50% that on land. Furthermore, we hypothesized that varying body position would cause substantial changes in task mechanical demands, reflected by marked alterations in shoulder moments, power and work. Specifically, we predicted that elevation and lowering of the arm would require respectively less and more work when sitting compared to supine.

2. Methods

2.1. Participants and numerical procedure

Eighteen adults (Table 1) with no history of upper extremity injury or pain provided written informed consent to participate in the study. Sample size was determined a priori, based on effect size from a pilot study comparing total mechanical work between positions ($d = 0.83$, $n = 5$). Power analysis (G*Power 3; Faul et al., 2007) revealed that 18 participants were needed to detect similar effects using two-tailed, paired t-tests with 90% power and 5% type I error rate. Procedures were approved by the University of Porto Institutional Review Board.

Participants' upper bodies were scanned with a Mephisto 3D scanner (4DDynamics, Antwerp, Belgium). Virtual geometries were then edited and converted into computer-aided design models prior to import into ANSYS® Fluent® Release 14.5 computational fluid dynamics software (ANSYS, Inc., Canonsburg, PA, USA). Individualized geometries have the advantage to make simulations sensitive to subtle interindividual differences in morphology (Lauer et al., 2016). Seven anatomical landmarks were located (see Fig. 1) to construct thorax and upper arm coordinate systems according to the ISB standards (Wu et al., 2005). Accurate knowledge of joint center location is essential to compute joint kinetics that can reliably and confidently be interpreted. Therefore, glenohumeral joint center was experimentally determined in a separate instance according to the procedure described in Lempereur et al. (2010). For that purpose, four additional markers placed distally

Table 1
Participant demographics. N: number of subjects. BMI: body mass index.

Gender	N	Age (years)		Height (m)		Mass (kg)		BMI ($kg \cdot m^{-2}$)	
		Mean	SD	Mean	SD	Mean	SD	Mean	SD
Female	7	30.8	9.6	1.63	0.06	58.1	9.3	21.8	3.2
Male	11	33.1	9.0	1.80	0.09	76.5	13.2	23.6	2.7

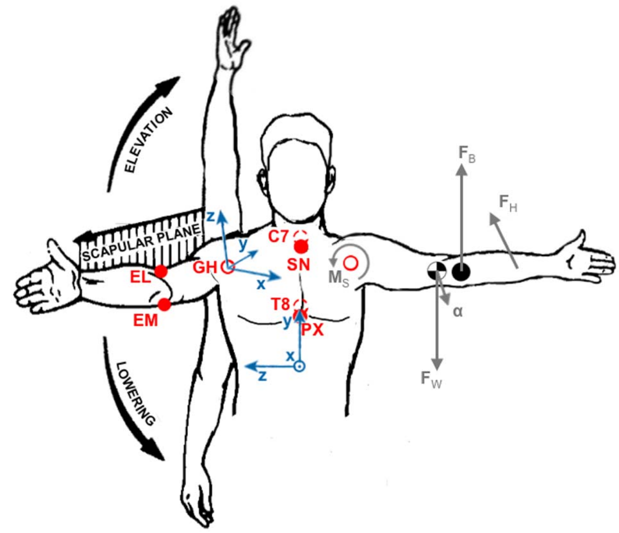

Fig. 1. Schema of the kinematics and inverse dynamics models. Continuous upper limb elevation and lowering were simulated in the scapular plane, set at an angle of 30° with the sagittal plane. The anatomical landmarks marked in red (EL: lateral epicondyle; EM: medial epicondyle; GH: glenohumeral joint center; SN: suprasternal notch; PX: xiphoid process; plus C7 and T8) were used to construct the upper limb and thorax right-handed coordinate systems (in blue). The latter is purposely represented at its wrong origin for readability. The external forces (weight, buoyancy, hydrodynamic force; $\mathbf{F}_W$, $\mathbf{F}_B$, $\mathbf{F}_H$) are denoted in gray. The resultant shoulder moment $\mathbf{M}_S$, calculated as the sum of the three other moments of force ($\mathbf{M}_W$, $\mathbf{M}_B$, $\mathbf{M}_H$), is the value of interest here. (For interpretation of the references to colour in this figure legend, the reader is referred to the web version of this article.)

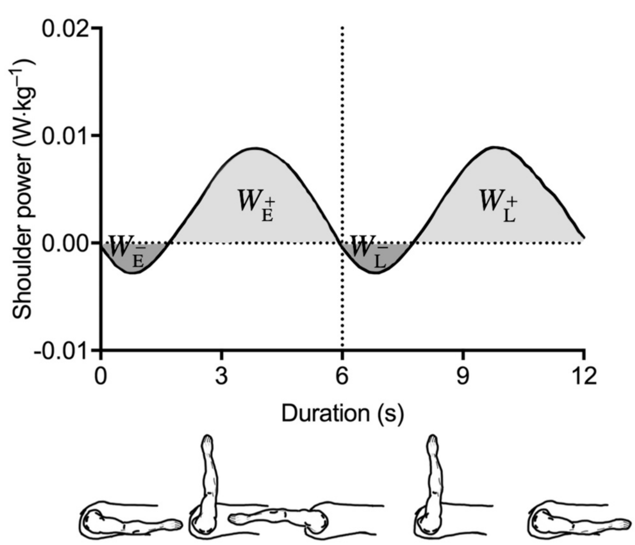

Fig. 2. Illustrative plot of instantaneous shoulder joint power during one complete cycle. Individual periods of negative (dark gray areas) and positive work (light gray areas) done at the shoulder are respectively labeled W^+ and W^-. Mechanical work values are computed separately for elevation (W_E) and lowering (W_L) by integration of the power time series with respect to time. The vertical dotted line indicates the transition from elevation to lowering of the upper limb, as exemplified by the drawing.

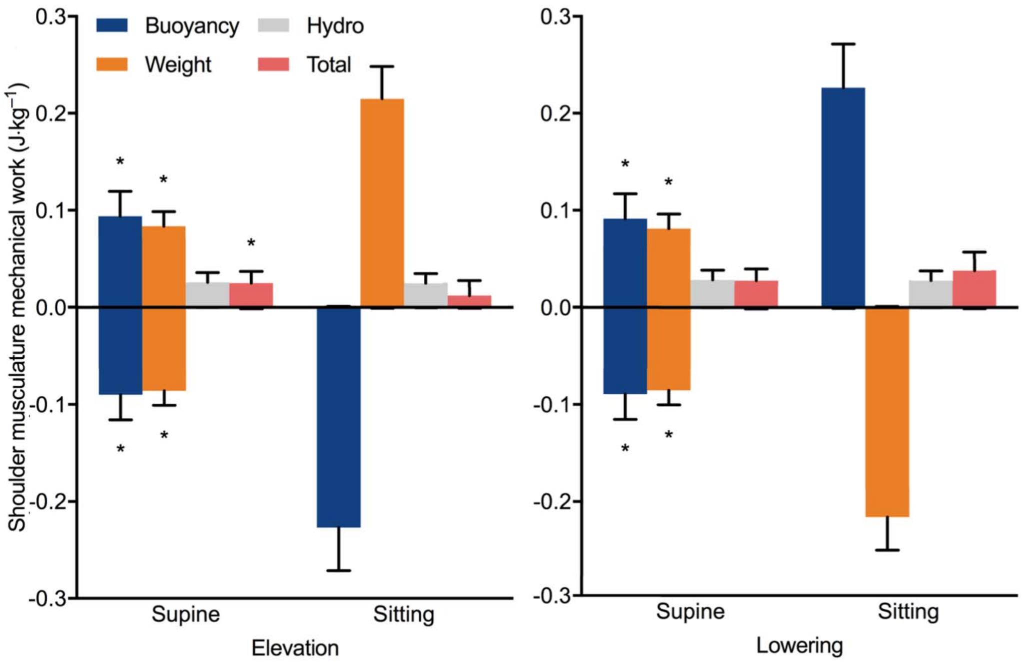

Fig. 3. Average mechanical work done during aquatic scapular plane arm elevation (left panel) and lowering (right panel). Work has been further broken down into individual components related to external forces (buoyancy, weight, and hydrodynamic force). Data are means (SD) * Significantly different ($P < 0.05$) from the value in sitting position.

on the upper arm were tracked as participants were performing three repetitions of flexion/extension, abduction/adduction and circumduction. This yielded a set of vectors rotating over time, from which the glenohumeral joint center was reconstructed using Gamage and Lasenby's least squares algorithm (Gamage and Lasenby, 2002).

Arm elevation and lowering in the scapular plane were numerically simulated in Fluent to evaluate instantaneous hydrodynamic forces. The upper limb was animated in the glenohumeral neutral ("full can") position at 30°/s via a custom dynamic mesh algorithm to ensure smooth, skin-like mesh deformation and simulation convergence. The surface of the virtual models was meshed with ~40,000 mm-scale triangular faces onto which Fluent flow solver computed pressure and shear stress at each time step.

2.2. Inverse dynamics modeling

Net shoulder moment calculations were based on Euler's second law of motion for rigid body dynamics, the general form of which is:

$$\mathbf{M}_{\mathrm{S}} = I\boldsymbol{\alpha} - \mathbf{M}_{\mathrm{W}} - \mathbf{M}_{\mathrm{B}} - \mathbf{M}_{\mathrm{H}}, \tag{1}$$

where $\mathbf{M}_s$ is the resultant shoulder moment; I, the moments of inertia of the upper limb; $\boldsymbol{\alpha}$, its angular acceleration; $\mathbf{M}_W$, $\mathbf{M}_B$, and $\mathbf{M}_H$, the moments of weight, buoyancy and hydrodynamic force about the glenohumeral joint center, computed as follows:

$$\mathbf{M}_{\mathrm{W}} = \mathbf{r}_{\mathrm{COM}} \times \mathbf{F}_{\mathrm{W}}, \tag{2}$$

$$\mathbf{M}_{\mathrm{B}} = \mathbf{r}_{\mathrm{COB}} \times \mathbf{F}_{\mathrm{B}}, \tag{3}$$

$$\mathbf{M}_{\mathrm{H}} = \sum_{i=1}^{n} \mathbf{r}_i \times \mathbf{F}_{\mathrm{H},i}, \tag{4}$$

where $\mathbf{r}_{COM}$ is the position vector of the upper limb's center of mass (relative to the glenohumeral joint center); $\mathbf{F}_W$, the upper limb's weight vector; $\mathbf{r}_{COB}$, the position vector of the upper limb's center of buoyancy; $\mathbf{F}_B$, the buoyant force vector; $\mathbf{r}_i$, the position vector of the centroid of face i at the surface of the upper limb virtual geometry; and $\mathbf{F}_{H,i}$, the sum of pressure and friction acting on the face i. Upper limb buoyancy and center of buoyancy location were obtained from the volume of the virtual model, whereas the upper limb mass, center of mass location and moments of inertia were estimated from scaling equations based on subject anthropometry (Dumas et al., 2007). In order to simulate the sitting position, weight and buoyancy vectors were rotated by 90°. The interested reader is referred to Lauer et al. (2016) for further details regarding numerical settings.

Shoulder moments were described in a non-orthogonal joint coordinate system to get a more coherent anatomical and clinical understanding of joint dynamics (Gagnon et al., 2001; Schache and Baker, 2007), and normalized to body weight times arm length (%BW·AL; Hof, 1996). By convention, positive joint moments were net mechanical actions of flexion, adduction and internal rotation of the shoulder.

2.3. Mechanical joint power and work computation

Instantaneous shoulder joint power was taken as the dot product of net shoulder moment and shoulder angular velocity vectors, and normalized to participants' body mass. Partitioning the instantaneous power into individual components related to hydrodynamic force, weight and buoyancy was computed likewise. The positive $W_{E/L}{}^{+}$ and negative mechanical work $W_{E/L}{}^{-}$ delivered at the shoulder joint during arm elevation and lowering in the scapular plane were computed as follows: power time series were individually integrated with respect to time over discrete periods of positive and negative power pertaining to arm elevation and lowering (see Fig. 2 for illustration), yielding $W_{E/L}{}^{+}$ and $W_{E/L}{}^{-}$ done by each force acting upon the upper limb during the corresponding phases. To assess the load during the same movement performed on land, $W_{E/L}{}^{+}$ and $W_{E/L}{}^{-}$ were recomputed once the contributions of hydrodynamic force and buoyancy subtracted.

2.4. Statistical analysis

Statistical analysis was run in R 3.3.2 (https://www.R-project.org/), with a significance level of 0.05. Assumption of normality was checked for all variables with the Shapiro–Wilk test prior to analysis. Means, standard deviations and 95% confidence intervals were computed. Existence of significant differences in peak moment and mechanical work between exercising positions were tested with Student's paired t-

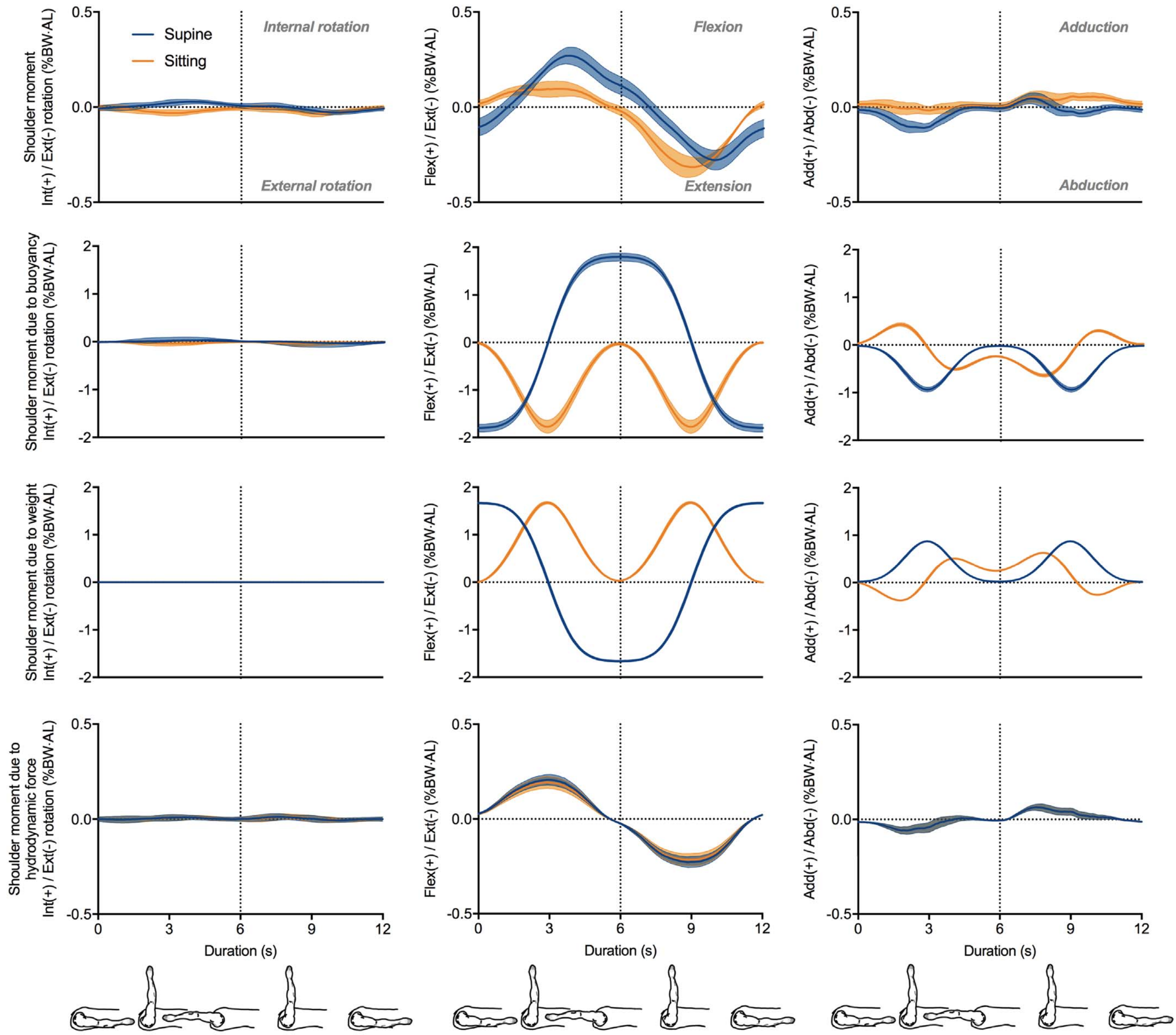

Fig. 4. Net shoulder joint moment (top row) and moments of external forces (three bottom rows) about internal/external rotation, flexion/extension, and adduction/abduction axes. The vertical dotted line indicates the transition from scapular plane abduction to adduction. Blue and orange traces respectively denote supine and sitting positions. Data are presented as means (thick lines) and 95% confidence bands (filled area). Note that top and bottom graphs were scaled down for better readability. (For interpretation of the references to colour in this figure legend, the reader is referred to the web version of this article.)

tests. No tests were run on power profiles since only their shape and polarity were of interest.

3. Results

3.1. Shoulder mechanical work

Positive mechanical work done at the shoulder was 32.4% (95% CI [29.2, 35.6]) and 25.0% [22.8, 27.2] that when performing the same movement on land, supine and sitting respectively. Arm elevation was less demanding sitting than supine (mean 0.012 (SD 0.018) vs mean 0.027 (SD 0.012) J·kg^{-1}, $P = 0.034$; Fig. 3), whereas the mechanical work done during arm lowering did not differ significantly between positions (mean 0.038 (SD 0.018) vs mean 0.027 (SD 0.012) J·kg^{-1}, $P = 0.062$). Significantly less work was done when supine compared to sitting against buoyancy (mean 0.092 (SD 0.026) vs mean 0.227 (SD 0.045) J·kg^{-1}, $P < 0.001$) and weight (mean 0.081 (SD 0.015) vs mean 0.215 (SD 0.034) J·kg^{-1}, $P < 0.001$). Work done against water resistance (mean 0.028 (SD 0.010) J·kg^{-1}) was unchanged by body position. Overall, little negative mechanical work was done at the shoulder (< 0.0009 J·kg^{-1}, or < 4% of the positive mechanical work done).

3.2. Net shoulder joint moments

Net shoulder moments about the axes of internal/external rotation and adduction/abduction were negligible in both positions. However, marked differences were observed about the axis of flexion/extension. Supine exhibited alternation of extension–flexion–extension moments, whereas sitting revealed a flattened flexion moment pattern during arm elevation (Fig. 4, first row). Symmetric profiles were seen for moments of weight and buoyancy, although the latter were higher in magnitude. Regardless of body position, moments of hydrodynamic force were null when the arm was either along the thigh or elevated along the head (0

Table 2
Means and 95% confidence intervals for moment peaks. $\mathbf{M}_{S,peak}$, $\mathbf{M}_{B,peak}$, $\mathbf{M}_{W,peak}$, and $\mathbf{M}_{H,peak}$ are peak values for net shoulder moment, and moments of buoyancy, weight, and hydrodynamic force. Peaks were identified during arm elevation and lowering about each rotation axis: internal/external rotation, flexion/extension, and adduction/abduction axes. Shaded rows indicate significant differences ($P < 0.05$) between performing supine and sitting.

		Elevation				Lowering			
Variable		Supine		Sitting		Supine		Sitting	
		Mean	95% CI	Mean	95% CI	Mean	95% CI	Mean	95% CI
$\mathbf{M}_{S,peak}$									
	Int(+)/Ext(−)	0.03	[0.02, 0.04]	−0.02	[−0.01, −0.03]	−0.01	[−0.01, −0.02]	−0.01	[−0.01, −0.02]
	Flex(+)/Ext(−)	0.27	[0.23, 0.31]	0.10	[0.06, 0.14]	−0.28	[−0.23, −0.33]	−0.32	[−0.26, −0.38]
	Add(+)/Abd(−)	−0.11	[−0.09, −0.13]	0.02	[0.01, 0.04]	0.05	[0.02, 0.08]	0.05	[0.02, 0.09]
$\mathbf{M}_{B,peak}$									
	Int(+)/Ext(−)	0.02	[0.01, 0.02]	−0.02	[−0.01, −0.02]	−0.02	[−0.01, −0.03]	−0.02	[−0.01, −0.03]
	Flex(+)/Ext(−)	± 1.80	[± 1.72, ± 1.88]	−1.77	[−1.64, −1.90]	± 1.80	[± 1.72, ± 1.88]	−1.77	[−1.64, −1.90]
	Add(+)/Abd(−)	−0.94	[−0.89, −0.99]	0.43	[0.40, 0.46]	−0.94	[−0.89, −0.99]	−0.64	[−0.61, −0.67]
$\mathbf{M}_{W,peak}$									
	Int(+)/Ext(−)	0	0	0	0	0	0	0	0
	Flex(+)/Ext(−)	± 1.67	[± 1.65, ± 1.69]	1.67	[1.65, 1.69]	± 1.67	[± 1.65, ± 1.69]	1.67	[1.65, 1.69]
	Add(+)/Abd(−)	0.87	[0.86, 0.88]	0.51	[0.50, 0.52]	0.87	[0.86, 0.88]	0.63	[0.62, 0.64]
$\mathbf{M}_{H,peak}$									
	Int(+)/Ext(−)	0.01	[0.00, 0.02]	0.01	[0.00, 0.02]	0.01	[0.00, 0.02]	0.01	[0.00, 0.02]
	Flex(+)/Ext(−)	0.21	[0.18, 0.23]	0.21	[0.18, 0.23]	−0.23	[−0.20, −0.26]	−0.23	[−0.20, −0.26]
	Add(+)/Abd(−)	−0.06	[−0.04, −0.08]	−0.06	[−0.04, −0.08]	0.06	[0.05, 0.08]	0.06	[0.05, 0.08]

or 180°), and peaked towards the middle of arm elevation and lowering. Means and 95% confidence intervals for moment peaks are displayed in Table 2. Buoyancy and weight moment peaks were significantly higher in magnitude when supine about the axis of adduction/abduction ($P < 0.001$). Net shoulder moment peaks were significantly higher when lying supine about flexion/extension and adduction/abduction during arm elevation only ($P < 0.001$).

3.3. Shoulder instantaneous power

Shoulder mechanical power output differed between the two exercising positions (Fig. 5). When supine, both scapular plane elevation and lowering required successively short period (~1.2 s) of negative power and longer period (~4.8 s) of positive power, peaking at 0.01 W·kg^{-1} towards 30 and 80% of the full motion. Conversely, when sitting, levels of power were 3× lower during elevation (0.003 W·kg^{-1}), and slightly higher during lowering (0.012 W·kg^{-1}). Total power was further partitioned into individual components related to buoyancy, weight, and hydrodynamic forces. Buoyancy and weight peak power was lower supine than sitting (0.05 vs 0.08 W·kg^{-1} and 0.04 vs 0.07 W·kg^{-1}, respectively). Patterns changed sign twice as frequently supine compared to sitting, whereas profiles of hydrodynamic force power were identical between positions.

4. Discussion

4.1. Water reduces mechanical demands on the shoulder by up to 75%

For the first time, this study reports a quantification of the mechanical demands on the shoulder of underwater scapular plane exercises. We observed a considerable three- to fourfold work reduction at the shoulder compared to the same movement on land, supporting our first hypothesis. This is strong mechanical evidence encouraging the early implementation of aquatic therapy during rehabilitation. EMG studies previously reached the same conclusion (Castillo-Lozano et al., 2014; Kelly et al., 2000), although the actual diminution of shoulder load could not be accurately evaluated. The protective nature of the aquatic environment was solely inferred from the observation that activity of the deltoid and rotator cuff muscles was less in water than on land.

The knowledge of joint work presents additional advantages. Unlike a given level of muscle activity, which may correspond to different load (Tax et al., 1990), joint work offers a robust measure of task mechanical demands (Winter, 2005). Furthermore, since mechanical work necessitates metabolic energy to be performed, it can be used as a physiological marker of intensity across a large variety of exercises. For example, considering the maximum mechanical work output observed during arm elevation (0.027 J·kg^{-1}, hence 1.9 J for an average 70-kg subject) and a conservative muscle efficiency of 0.25 (expected from the thermodynamics of muscle contraction; Woledge et al., 1985), we predict a metabolic cost of 7.6 J and metabolic work rate of 1.3 W. This is about 28× less than the energy needed to wash dishes (Jetté et al., 1990)!

4.2. Shoulder load during arm elevation can more than double when supine

Our second hypothesis was only partially supported by our data. Although the mechanical work during arm elevation performed sitting was less than half the work when supine, no differences were noted between positions during arm lowering. Thus, buoyancy alone fails to explain changes in shoulder load. This invalidates the straightforward analysis presented in Introduction, and rather suggests that a subtler interaction occurs between all external forces. Simply considering buoyancy while disregarding weight and hydrodynamic forces to make an educated guess about movement mechanics and clinical implications is potentially misleading (Prins and Cutner, 1999; Thein and Brody, 2000; Vo et al., 2013). Furthermore, substantial alteration in shoulder load may compromise therapy success. While exercising sitting may prove beneficial in very early rehabilitation stages of a weakened shoulder to restore joint mobility at low effort, mechanical solicitation might very well be too light to elicit active strength gain later on. Inversely, exercising supine seems more likely to be profitable at intermediate rehabilitation stages since task mechanical requirements were overall higher.

4.3. Inverse dynamics identifies the prime movers

Net shoulder moments were much higher about the flexion/extension axis than about the other two axes. Polarity of the net joint moment reflects the dominant muscle group during the observed motion

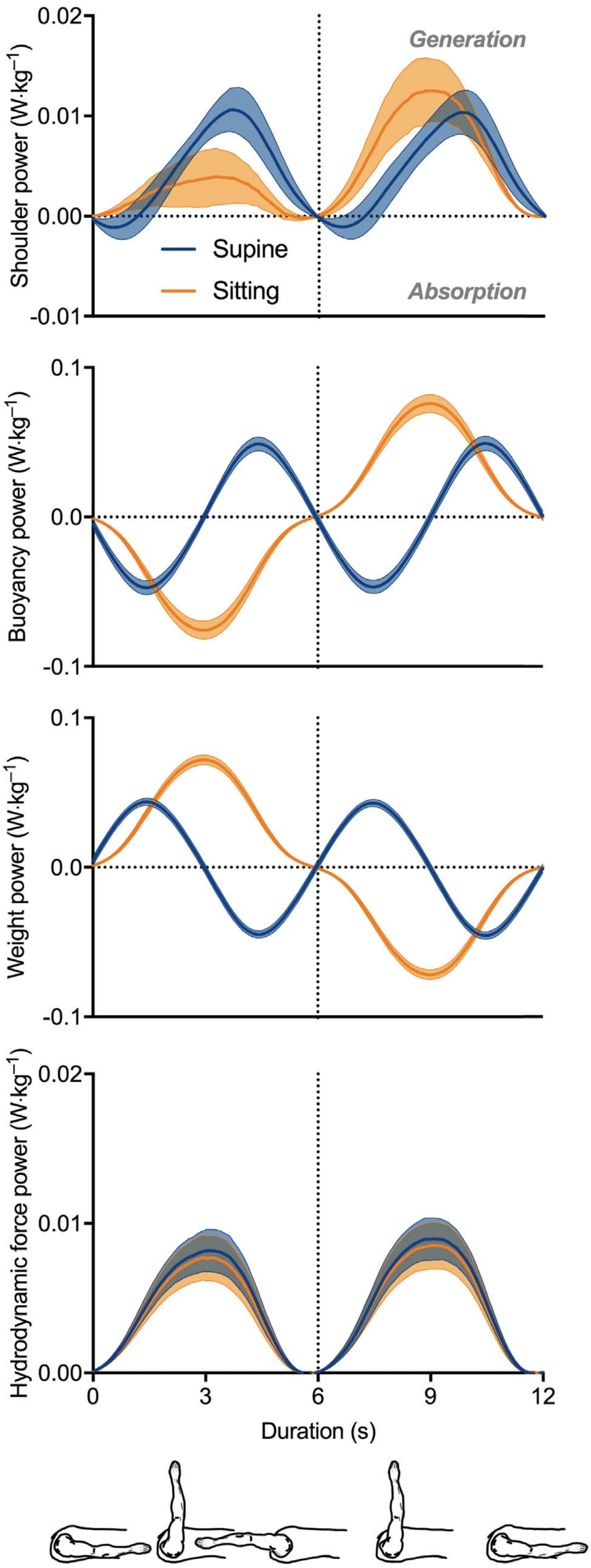

Fig. 5. Instantaneous power of shoulder musculature and external forces plotted against one cycle. Positive/negative power reflects production/absorption of mechanical energy through concentric/eccentric muscle action. See Fig. 4 for colour legend. Note that top and bottom graphs were plotted on different scales for better readability.

(Winter, 2005). Shoulder flexors and extensors therefore prevailed during elevation and lowering of the arm in the scapular plane; in contrast, internal/external rotators and adductors/abductors had little to no net mechanical outcome. This is consistent with reports of high activation levels (relative to the other muscles studied) of the pectoralis major and anterior deltoid, and silent subscapularis and posterior deltoid (Castillo-Lozano et al., 2014; Kelly et al., 2000). Surprisingly though, Kelly et al. had found that the first and third most recruited muscles were the supraspinatus and infraspinatus (Kelly et al., 2000), which respectively act as shoulder abductor and external rotator. The solution to this paradox likely lies in the dual action of the pectoralis major: as it raises the arm, it also produces an undesired adduction moment component that must be counteracted by other muscles in order to provide joint stability (Veeger and van der Helm, 2007). Two important consequences follow. First, EMG improperly identifies the prime movers. Second, inverse dynamics does inform about shoulder load but gives little insight into individual muscle function, particularly those cocontracting. Examining individual muscle contributions to total mechanical demands in water would require very elaborate musculoskeletal models, which is a step we are currently exploring.

4.4. Body position determines muscle contraction type

Shoulder power was alternately negative (shortly after movement reversal) and positive when supine, whereas it was constantly positive when sitting. Robertson and Winter postulated that a positive/negative joint power reflects the production/absorption of mechanical energy through concentric/eccentric contractions (Robertson and Winter, 1980). Recently, the reliability of joint power analysis in proximal muscle groups with relatively short tendons (such as at the shoulder) has gained experimental support (Cronin et al., 2013). This is important because the identification of muscle contraction type is not easily accessible in vivo on land, and even less so in water. Scapular plane exercises when sitting were therefore purely concentric, whereas they required rapid pre-stretch followed by concentric force production when supine.

In fast ($>300°/s$) underwater knee exercises, eccentric contraction was found to result from interaction between the moving limb and accelerated masses of water (Pöyhönen et al., 2001). Here, this cannot be the case; energy absorption would have occurred before movement reversal to slow the upper limb down, which is likely unnecessary at 30°/s. Inspection of moment and power traces reveal that energy absorption rather coincides with high moment of buoyancy tending to pull the arm upward and very small moment of hydrodynamic force. Most importantly, this means that eccentric contraction can be elicited at $10\times$ slower speeds without buoyant devices by designing the exercise in such a way that the arm passes the horizontal when the flow has not fully developed, typically at the onset of the transition between elevation and lowering.

4.5. Inter-individual differences in buoyancy has the most notable effect on shoulder load

In silico evaluation of shoulder mechanical loading allowed us to simulate identical isokinetic shoulder movements across participants. In other words, inter-individual variability in kinematical pattern was eliminated, isolating the effect of morphological differences on shoulder load. We reasoned that the first could, in practice, be kept low by observing task amplitude and speed instructions, whereas the second is often overlooked and can hardly be monitored. It was thus felt that our simplification could address a more pressing need for understanding the extent to which human body design influences force production in water and clinical implications.

Individuals with varying body composition and shape naturally show different floating ability and resistance to movement. Very lean individuals may have upper limbs that sink. Furthermore, tall individuals generally have longer segments, hence larger surface area in contact with water. Although body fat was not measured, our sample was representative of healthy and overweight individuals based on BMI in the range 19–30. Judging from standard deviations of mechanical work when sitting, variability in shoulder load had more to do with inter-individual differences in upper limb buoyancy (SD 0.045) than hydrodynamic force (SD 0.010). Therefore, care should be taken in extrapolating our findings to underweight or obese patients as we can reasonably expect marked changes in kinetic patterns.

5. Conclusions

Coupling inverse dynamics with numerical fluid flow simulations offers the first thorough non-invasive evaluation of musculoskeletal system loading in water. The work done by shoulder muscles is ~3–4× less in water than on land, providing strong mechanical evidence in support of the inclusion of slow aquatic exercises in postoperative shoulder rehabilitation. Furthermore, important consequences for informed design of aquatic rehabilitation protocols were drawn. Joint moments reveal that EMG measures are inappropriate to understand which muscle groups are the most loaded. Furthermore, varying body position in water does have a substantial impact on muscle function, eliciting purely concentric contractions when sitting and short period of stretch when supine. Clinicians are encouraged to provide rigorous task instructions in order to target the desired outcome, and to rely on EMG findings with caution. Inverse dynamics in water, along with actual kinematics recording via markerless techniques, is expected to significantly reshape the way aquatic exercises are planned, joint work and joint moment being ideal candidates to assess exercise intensity and establish treatment guidelines and best practices.

References

Agence Technique de l'Information sur l'Hospitalisation, 2017. URL. http://www.atih.sante.fr, Accessed date: 8 May 2017.
Biscarini, A., Cerulli, G., 2007. Modeling of the knee joint load in rehabilitative knee extension exercises under water. J. Biomech. 40, 345–355.
Brady, B., Redfern, J., MacDougal, G., Williams, J., 2008. The addition of aquatic therapy to rehabilitation following surgical rotator cuff repair: a feasibility study. Physiother. Res. Int. 13, 153–161.
Castillo-Lozano, R., Cuesta-Vargas, A., Gabel, C.P., 2014. Analysis of arm elevation muscle activity through different movement planes and speeds during in-water and dry-land exercise. J. Shoulder Elb. Surg. 23, 159–165.
Cronin, N.J., Prilutsky, B.I., Lichtwark, G.A., Maas, H., 2013. Does ankle joint power reflect type of muscle action of soleus and gastrocnemius during walking in cats and humans? J. Biomech. 46, 1383–1386.
Desroches, G., Chèze, L., Dumas, R., 2010. Expression of joint moment in the joint coordinate system. J. Biomech. Eng. 132, 114503.
Dumas, R., Chèze, L., Verriest, J.-P., 2007. Adjustments to McConville et al. and Young et al. body segment inertial parameters. J. Biomech. 40, 543–553.
Faul, F., Erdfelder, E., Lang, A.-G., Buchner, A., 2007. G*power 3: a flexible statistical power analysis program for the social, behavioral, and biomedical sciences. Behav. Res. Methods 39, 175–191.
Gagnon, M., Desjardins, P., Larrivé, A., 2001. Joint coordinate systems of axes for coherence in reporting kinematic and kinetic data. Clin. Biomech. 16, 349–350.
Gamage, S.S.H.U., Lasenby, J., 2002. New least squares solutions for estimating the average centre of rotation and the axis of rotation. J. Biomech. 35, 87–93.
Hof, A.L., 1996. Scaling gait data to body size. Gait Posture 4, 222–223.
Jetté, M., Sidney, K., Blümchen, G., 1990. Metabolic equivalents (METS) in exercise testing, exercise prescription, and evaluation of functional capacity. Clin. Cardiol. 13, 555–565.
Kelly, B.T., Roskin, L.A., Kirkendall, D.T., Speer, K.P., 2000. Shoulder muscle activation during aquatic and dry land exercises in nonimpaired subjects. J. Orthop. Sports Phys. Ther. 30, 204–210.
Kristianslund, E., Krosshaug, T., Mok, K.-M., McLean, S., van den Bogert, A.J., 2014. Expressing the joint moments of drop jumps and sidestep cutting in different reference frames–does it matter? J. Biomech. 47, 193–199.
Lauer, J., Rouard, A.H., Vilas-Boas, J.P., 2016. Upper limb joint forces and moments during underwater cyclical movements. J. Biomech. 49, 3355–3361.
Lempereur, M., Leboeuf, F., Brochard, S., Rousset, J., Burdin, V., Rémy-Néris, O., 2010. In vivo estimation of the glenohumeral joint centre by functional methods: accuracy and repeatability assessment. J. Biomech. 43, 370–374.
Pöyhönen, T., Keskinen, K.L., Kyröläinen, H., Hautala, A., Savolainen, J., Mälkiä, E., 2001. Neuromuscular function during therapeutic knee exercise under water and on dry land. Arch. Phys. Med. Rehabil. 82, 1446–1452.
Prins, J., Cutner, D., 1999. Aquatic therapy in the rehabilitation of athletic injuries. Clin. Sports Med. 18, 447–461.
Robertson, D.G., Winter, D.A., 1980. Mechanical energy generation, absorption and transfer amongst segments during walking. J. Biomech. 13, 845–854.
Sasaki, K., Neptune, R.R., Kautz, S.A., 2009. The relationships between muscle, external, internal and joint mechanical work during normal walking. J. Exp. Biol. 212, 738–744.
Schache, A.G., Baker, R., 2007. On the expression of joint moments during gait. Gait Posture 25, 440–452.
Tax, A.A., van der Gon Denier, J.J., Erkelens, C.J., 1990. Differences in coordination of elbow flexor muscles in force tasks and in movement tasks. Exp. Brain Res. 81, 567–572.
Thein, J.M., Brody, L.T., 2000. Aquatic-based rehabilitation and training for the shoulder. J. Athl. Train. 35, 382–389.
Thigpen, C.A., Shaffer, M.A., Gaunt, B.W., Leggin, B.G., Williams, G.R., Wilcox 3rd, R.B., 2016. The American Society of Shoulder and Elbow Therapists' consensus statement on rehabilitation following arthroscopic rotator cuff repair. J. Shoulder Elb. Surg. 25, 521–535.
van den Bogert, A.J., 1994. Analysis and simulation of mechanical loads on the human musculoskeletal system: a methodological overview. Exerc. Sport Sci. Rev. 22, 23–51.
Veeger, H.E.J., van der Helm, F.C.T., 2007. Shoulder function: the perfect compromise between mobility and stability. J. Biomech. 40, 2119–2129.
Vo, A., Zhou, H., Dumont, G., Fogerty, S., Rosso, C., Li, X., 2013. Physical therapy and rehabilitation after rotator cuff repair: a review of current concepts. Int. J. Phys. Med. Rehabil. 1, 142.
Winby, C.R., Gerus, P., Kirk, T.B., Lloyd, D.G., 2013. Correlation between EMG-based co-activation measures and medial and lateral compartment loads of the knee during gait. Clin. Biomech. 28, 1014–1019.
Winter, D.A., 2005. Biomechanics and Motor Control of Human Movement, 3rd ed. John Wiley & Sons, Hoboken, NJ.
Woledge, R.C., Curtin, N.A., Homsher, E., 1985. Energetic Aspects of Muscle Contraction. Academic Press, Orlando, FL.
Wu, G., van der Helm, F.C.T., Veeger, H.E.J.D., Makhsous, M., Van Roy, P., Anglin, C., Nagels, J., Karduna, A.R., McQuade, K.J., Wang, X., Werner, F.W., Buchholz, B., Biomechanics, I.S.O., 2005. ISB recommendation on definitions of joint coordinate systems of various joints for the reporting of human joint motion–part II: shoulder, elbow, wrist and hand. J. Biomech. 38, 981–992.
Zajac, F.E., Neptune, R.R., Kautz, S.A., 2002. Biomechanics and muscle coordination of human walking. Part I: introduction to concepts, power transfer, dynamics and simulations. Gait Posture 16, 215–232.